JOURNAL OF CATALYSIS **167,** 127–141 (1997)
ARTICLE NO. CA971520

Catalytic Reduction of Nitrogen Oxides by Olefins in the Presence of Oxygen over Copper/Alumina: Influence of Copper Loading and Formation of Byproducts

Frank Radtke, René A. Koeppel, Elio G. Minardi, and Alfons Baiker[1]

Department of Chemical Engineering and Industrial Chemistry, Swiss Federal Institute of Technology, ETH-Zentrum, CH-8092 Zurich, Switzerland

Received May 9, 1996; revised September 16, 1996; accepted October 31, 1996

The performance of copper/alumina in the selective catalytic reduction of NO_x by olefins in excess oxygen has been studied by means of FTIR gas phase analysis. Special emphasis was devoted to the formation of harmful byproducts such as N_2O, HCN, and NH_3. The effect of copper loading, reaction temperature, nitrogen oxides (NO, NO_2), hydrocarbons (ethene, propene), and water on activity and on the formation of byproducts has been investigated. Increasing the copper loading from 0.46 to 1.65 wt% CuO resulted in a shift of the maximum activity to lower temperatures and in slightly lower nitrogen yields. NO_2 was reduced more efficiently than NO with both reductants, whereas no significant difference in activity was observed when either ethene or propene was used as a reductant. Water addition suppressed catalytic activity and leveled off the influence of copper loading. Substantial amounts of N_2O, HCN, and NH_3 were observed for copper-containing catalysts, with ethene showing a markedly lower tendency to form HCN and N_2O. Addition of water to the feeds eliminated HCN formation and suppressed the production of N_2O but had only a marginal effect on NH_3 formation. Temperature-programmed surface reaction (TPSR) and *in situ* FTIR experiments in various atmospheres with catalysts loaded under reaction conditions with dry feeds revealed the presence of surface deposits containing precursor species for ammonia and hydrogen cyanide formation. No such species were found when catalysts were loaded with feeds containing water. Reference TPSR measurements with acetonitrile and ethyl isocyanate in oxygen- and/or water-containing atmospheres showed a temperature dependence of ammonia formation comparable to that observed for the loaded catalyst, giving evidence that nitrile as well as isocyanate intermediates formed on the catalyst surface could be the source of ammonia found in catalytic activity testing. FTIR spectroscopy revealed the presence of nitrogen-containing surface species for catalysts loaded with a dry feed containing NO and propene, while no such species were found when wet feeds were used. Upon heating in H_2/N_2, cyanide species were produced, whereas isocyanate surface intermediates appeared in the spectra after heating in O_2/N_2. The findings are in accordance with a mechanism in which a nitrogen-containing precursor, which can be a nitrile or an oxime species, reacts to surface isocyanate and/or cyanide species. Hydrolysis of these intermediates provides a pathway to NH_3. © 1997 Academic Press

INTRODUCTION

Stringent emission control requirements have stimulated the development of various NO_x control technologies over the last few decades. For stationary NO_x sources such as power plants, and for mobile sources such as gasoline fueled engines working under stoichiometric air/fuel ratios, technical solutions are available (1, 2). Recently, diesel and lean-burn gasoline fueled engines have attracted considerable attention due to their high fuel efficiency and thus lower emission of carbon dioxide. These types of engines present new challenges for NO_x emission control, as they generally operate under net oxidizing conditions under which typical three-way catalysts show little activity towards NO_x reduction (1, 2). As NH_3 is not suitable for application as a reducing agent in motor vehicles, increased effort has been put into the development of suitable catalysts capable of reducing nitrogen oxides in the presence of oxygen with hydrocarbons as reducing agents (2–4).

Besides the widely investigated zeolite-based catalysts (3–18), metal oxides, with and without transition metal additives (19–39), have been reported to be active for this reaction. Among the most active materials evaluated to date are metal ion exchanged zeolites, but these materials have shown limited hydrothermal stability, whereas supported noble metal catalysts, active at low temperatures, produce substantial amounts of N_2O. In order to make application feasible, high space velocity performance, selectivity behavior, and durability of the lean NO_x catalysts in the presence of steam and sulfur oxides need to be improved.

Although many studies report the major nitrogen-containing product from NO_x reduction by hydrocarbons as being N_2, other species such as NH_3 (16, 17, 35), HCN (10, 12, 15–17, 35), HNCO (16, 17), N_2O (15–17), and aliphatic cyanide species (41) have been observed in the gas phase. Recently, a number of reports have appeared in the literature emphasizing the role of surface species in the course of the catalytic reduction of nitrogen oxides by hydrocarbons and several reaction mechanisms involving different reaction intermediates, e.g., oxygenated hydrocarbons

---

[1] To whom correspondence should be addressed.

0021-9517/97 $25.00

(5, 19, 20), NO_2 (30, 33), organic nitro or nitrite compounds (10, 12, 15, 37), surface isocyanate species (8, 13, 21, 24, 28, 36), and ammonia (18), have been proposed. Carbonaceous or coke deposits (5, 6, 32) which promote NO_x reduction have also been considered as reactive intermediates, whereas Cho (14) and Burch *et al.* (7, 11, 38) have proposed a redox type mechanism with the direct decomposition of NO as the crucial step.

Several studies have been reported in which the course of the reaction has been followed by infrared spectroscopy. These investigations have been concerned mainly with the formation and removal of surface isocyanate species (8, 21, 24, 28, 36, 39). Ukisu *et al.* (21, 22, 24) recently observed IR bands ascribable to adsorbed nitrogen-containing species such as isocyanates and cyanides on Cu/Al_2O_3 and $CuCs/Al_2O_3$ catalysts in the reduction of NO by propene in the presence of oxygen. Adsorbed water or hydroxyl groups on the catalyst surface suppressed the formation of the isocyanate species.

The formation of NCO surface species during NO_x reduction by hydrocarbons over supported catalysts seems well established. However, their role in the course of the reaction and in the formation of gaseous byproducts such as ammonia (16, 35) is not yet known and little information is available regarding the nature and the type of other adsorbates and their role in the formation of products during NO_x–hydrocarbon reaction.

In this paper we report the influence of copper loading on the catalytic activity of copper/alumina in the reduction of NO_x by olefins in the presence of oxygen. The effect of reaction temperature, nitrogen oxides (NO, NO_2), hydrocarbons (ethene, propene), and water on activity and on the formation of byproducts is investigated. The objective of the study was to obtain information on the nature and reactivity of surface species formed under reaction conditions. *In situ* infrared spectroscopy and temperature-programmed surface reactions (TPSR) of adsorbed species in different atmospheres were used to investigate the IR characteristics and reactivity of adsorbates formed under reaction conditions.

EXPERIMENTAL

Catalysts

Copper oxide/alumina catalysts with different CuO loadings were prepared by an impregnation method. Commercially available γ-Al_2O_3 (Alumina-C, Degussa Corp.) was agglomerated with water and dried at 363 K and 125 mbar to facilitate the handling of the material during preparation. The crushed alumina agglomerates were suspended in deionized water and a solution of $Cu(NO_3)_2 \cdot 3H_2O$ was slowly added. The resulting paste was dried for 12 h at 393 K and 125 mbar and calcined in air at 873 K for 2 h. The calcination temperature was determined by DTA/TG experiments to ensure complete decomposition of nitrate residuals. The final catalysts were crushed to a grain size of 120–250 μm. The copper loadings of the resulting catalysts, as determined by atomic absorption spectroscopy (AAS), amounted to 0.46, 0.78, and 1.65 wt%, respectively. The catalysts are denoted as CuO(0.46), CuO(0.78) and CuO(1.65) throughout the work.

BET measurements indicated that the impregnation procedure had little influence on the surface area of the γ-Al_2O_3 support (109 m^2/g_{Cat}, which decreased to 105 ± 2 m^2/g_{Cat} upon CuO loading). XRD analysis of Al_2O_3 and of the CuO/Al_2O_3 catalysts showed only reflections due to γ-alumina for all samples. No indication of the presence of crystalline CuO was found. Further investigation by temperature-programmed reduction (TPR) and thermoanalytical methods (TG/DTA) of the catalyst with the highest copper loading gave no evidence for the reduction of CuO up to 873 K. Temperature-programmed desorption of ammonia (NH_3-TPD) on alumina and the CuO/Al_2O_3 samples was performed with a FTIR instrument (Perkin–Elmer 1710) equipped with a DRIFT cell (controlled environmental chamber) and a mass spectrometer (42). Prior to measurement, the samples were pretreated by heating in a flow of 7.2% O_2/Ar at 423 K for 1 h. After cooling to ambient temperature, the samples were exposed to 3600 ppm NH_3 in Ar (50 ml(STP)/min) for 30 min. Physisorbed ammonia was removed by flushing with Ar (50 ml(STP)/min) for 30 min. The temperature was increased to 573 K at a rate of 7 K/min and FTIR spectra were recorded. Results depicted in Fig. 1 indicate a substantially higher proportion of Lewis acid sites (1625 cm^{-1}) with increasing copper loading, whereas the Brønsted acid sites (1485 and 1685 cm^{-1}) remained almost constant.

Apparatus

Catalytic measurements were performed on a fully computer-controlled microreactor system, which has been described in detail in Ref. (17). The apparatus consisted essentially of a gas mixing manifold, a U-tube quartz glass reactor (i.d. 6 mm), and a FTIR spectrometer for gas analysis. The reactant gas feeds, as specified in Table 1, were mixed by means of mass flow controllers (Brooks 5850E). The purities of the component gases, as specified by the supplier (Pan Gas), were: O_2 (99.999%), N_2 (99.995%), 9.9% CO (99.9%) in nitrogen, 5.03% C_2H_4 (99.5%) in nitrogen, 10% C_3H_6 (99.5%) in nitrogen, 4.9% NO (99.0%) in nitrogen. All gases were used without further purification. Water could be injected optionally into the gas stream through a microcapillary by means of a microstep pump.

The Fourier transform IR (FTIR) spectrometer (Bruker IFS 66) used for gas analysis at the reactor inlet and outlet was equipped with a heatable gas cell (100 ml volume; Infrared Analysis Inc.) and a MCT detector. To avoid condensation in the system, the gas cell and all tubings were

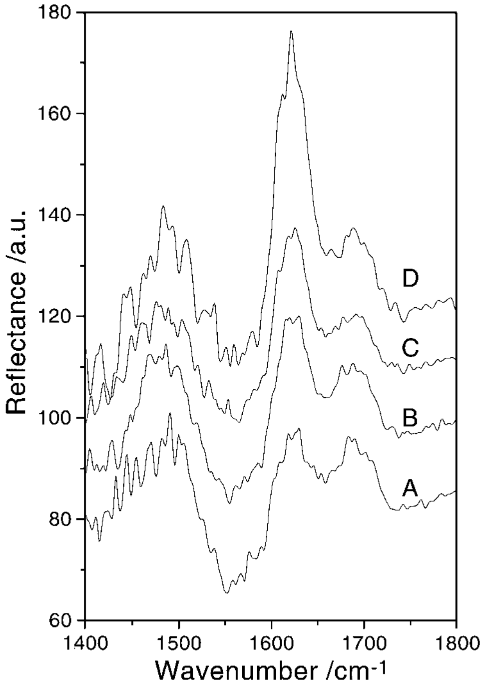

FIG. 1. IR absorption bands of surface-bound ammonia at 343 K for (A) Al_2O_3, (B) CuO(0.46), (C) CuO(0.78), and (D) CuO(1.65) after adsorption of 3600 ppm NH_3 in argon at room temperature and subsequent heating (7 K/min) in argon (50 ml(STP)/min).

heated at 393 K. Concentrations of each component were obtained by integration of specific absorption frequencies, using an appropriate software package (OPUS version 2.0; Bruker). For calibration, absorbance FTIR spectra (resolution 0.5 cm^{-1}, 50 scans per spectrum) of known concentrations were recorded for each component: NO, NO_2, N_2O, NH_3, HCN, C_2H_4, C_3H_6, CO, CO_2, and H_2O. Nitrogen was used for the background spectra. The accuracy in the concentration measurements by FTIR was ±5% for all components. The concentration of nitrogen formed by reduction of NO_x was calculated by using a mass balance over all nitrogen-containing species (NO, NO_2, N_2O, NH_3, and HCN). The selectivity to N_2 is calculated according to $S_N = 1 - [\Sigma \text{ N-products}]/[(NO_x)_{in} - (NO_x)_{out}]$, where NO_x is the sum of NO and NO_2, and Σ N-products represents all nitrogen-containing products except N_2.

TABLE 1

Simulated Exhaust Compositions (Feed Gas Mixtures) Used in Catalytic Studies: Balance Nitrogen

Feed[a]	NO [ppm]	NO_2 [ppm]	C_2H_4 [ppm]	C_3H_6 [ppm]	O_2 [%]	H_2O [%]
1 (1w)	980 (940)	0	0	910 (860)	2.0 (2.0)	0 (10)
2 (2w)	920 (940)	0	1290 (1260)	0	2.0 (2.0)	0 (10)
3 (3w)	0	970 (940)	0	910 (860)	1.9 (2.0)	0 (10)
4 (4w)	0	980 (950)	1450 (1270)	0	1.9 (2.0)	0 (10)

[a] Values in parentheses correspond to feeds containing 10% water, which are denoted with w.

Catalytic Tests

Standard experiments were carried out at atmospheric pressure using 250 mg of catalyst (120–250 μm sieve fraction). Before measurements, the samples were pretreated at 873 K for 2 h with 5% oxygen in nitrogen (150 ml(STP)/min) and then cooled to 473 K. Subsequently the reactant gas mixture, as specified in Table 1, was passed through the catalyst bed with a flow rate of 150 ml(STP)/min ($W/F = 0.1$ g s ml^{-1}) for 2 h. Steady-state measurements of the temperature dependence of the catalytic behavior were performed by raising the temperature in steps of 50 K from 473 to 873 K, with a typical duration of the isothermal steps of 80 min (dry feeds) and 110 min (wet feeds).

Temperature-Programmed Surface Reaction of Adsorbed Species (TPSR)

TPSR experiments were performed *in situ* with sample CuO(0.78) after standard pretreatment (2 h at 873 K in 5% O_2/N_2) and catalytic tests with Feed 1 (see Table 1) for 2 h at different temperatures (562, 615, 661 K). Subsequently, the feed gas was changed to nitrogen and the catalyst was rapidly cooled to 423 K. After thermal stability was reached, the temperature was raised to 900 K at 10 K/min in various atmospheres: (1) 2% O_2/N_2, (2) 2% H_2O/N_2, (3) 2% $H_2O + 2\%\ O_2/N_2$, and (4) 2% H_2/N_2. The concentrations of the evolving gas phase products were monitored by FTIR as described in Apparatus. Additional experiments were conducted by loading catalyst CuO(0.78) with Feed 1w and Feed 2, respectively, at 615 K.

For comparison, a series of TPSR experiments was carried out in the same temperature range with CuO(0.78) pretreated with 5% O_2/N_2 at 873 K for 2 h and then cooled to 423 K, using atmospheres as specified above containing additionally 200 ppm HCN, 212 ppm CH_3CN, or 1000 ppm C_2H_5NCO. Further information will be given in conjunction with the experimental results. Note that the concentrations analyzed by FTIR do not exactly reflect the concentration at a specific temperature due to the time delay in recording the spectra. As 200 s were needed to record a spectrum the measured gas phase concentrations represent a temperature range of about 30 K. Backmixing in the tubing between sample and detector could be excluded. However, possible influences by intraparticular diffusion and readsorption could not be ruled out completely under the conditions of TPSR measurements.

Diffuse Reflectance Infrared Fourier Transform (DRIFT) Measurements

DRIFT experiments were performed using a Bruker IFS 55 FTIR spectrometer equipped with a controlled environmental chamber fitted with ZnSe windows within a diffuse reflectance unit (both Spectra-Tech) and a nitrogen-cooled MCT detector. A more detailed description of the experimental setup is given in Ref. (43).

DRIFT measurements during temperature-programmed experiments were carried out with catalyst CuO(0.78) loaded at 615 K with Feed 1 and Feed 1w, respectively, and rapidly cooled in nitrogen to room temperature. The loaded samples were pretreated *in situ* in the FTIR chamber at 423 K in nitrogen (50 ml(STP)/min) for 1 h and a spectrum of the sample held at 423 K was taken as a reference (R_0) spectrum (resolution 4 cm^{-1}, 1000 scans). DRIFT spectra (4 cm^{-1}, 256 scans) were recorded after switching to the reaction gas mixture and increasing the temperature to 773 K in steps of 10 K. Defined flows (50 ml(STP)/min) of 5% O_2 (TPO) and 5% H_2 (TPR) in nitrogen, respectively, were used as reactant mixtures. Note that positive reflectances (i.e., increased reflectance R with respect to the background R_0) indicate disappearing surface species, whereas negative reflectances represent species formed. Reference spectra of pure compounds were measured on CuO(0.78) pretreated *in situ* in N_2 at 573 K for 30 min and cooled to 423 K, where background spectra (1000 scans) were taken. Following adsorption of CO, HCN, CH_3CN, and C_2H_5NCO, and after constant absorbances were reached (256 scans), the flow was switched to N_2 (50 ml(STP)/min) and additional spectra were recorded while the temperature was increased in steps of 10 K.

RESULTS

Catalytic Activity and Formation of Byproducts

Reduction of NO by propene. Figure 2A depicts the influence of copper loading on the temperature dependence of N_2 formation for the reduction of NO by propene (Feed 1). With increasing CuO loading, the catalysts reached maximum activity at lower temperature. For pure alumina the onset temperature of N_2 formation is at markedly higher temperature and no maximum is reached in the temperature range investigated. The maximum yield of nitrogen slightly decreases from 66% at 807 K for CuO(0.46) to 59% at 710 K for CuO(1.65). Similar behavior is found for the dependence of propene oxidation from copper loading. Complete olefin oxidation occurred at the same temperature where maximum N_2 yield was observed, with CO_2 and H_2O being the only oxidation products detected. In contrast, propene conversion over alumina did not exceed 50% at 863 K, thus producing almost equal amounts of CO and CO_2. With water in the feed (Feed 1w) the influence of Cu loading on NO conversion to N_2 was less pronounced, as can be seen from Fig. 2B. Compared to the dry feed maximum, NO conversion to N_2 decreased by approx. 20% to ca. 45% for the copper-containing samples. Interestingly, the temperature of maximum activity of CuO(0.46) decreased in the presence of water from 805 to 756 K, whereas it remained constant for the other catalysts. A substantial loss in activity is observed for alumina when a wet feed is used, resulting in only 12% N_2 yield at 863 K.

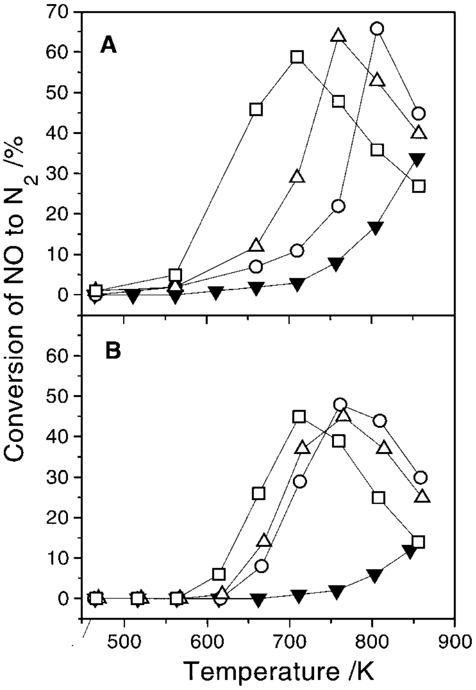

FIG. 2. Conversion of NO to nitrogen as a function of temperature for (A) Feed 1 and (B) Feed 1w: (▼) Al_2O_3, (○) CuO(0.46), (△) CuO(0.78), and (□) CuO(1.65); total flow rate, 150 ml(STP)/min; catalyst weight, 250 mg.

Regarding the formation of nitrogen-containing byproducts, different behavior emerged for N_2O and HCN. The formation of nitrous oxide as a function of the temperature is shown in Fig. 3A for Feed 1. N_2O formation was negligible over alumina. With increasing copper loading the formation of nitrous oxide significantly increased, reaching 31 ppm at 709 K for CuO(1.65). Addition of water to the feed gas (Feed 1w) suppressed the formation of N_2O to less than 5 ppm. Opposite behavior was observed for the formation of hydrogen cyanide (Fig. 3B). Substantial amounts of HCN were formed over alumina (22 ppm at 863 K) and CuO(0.46) (46 ppm at 765 K), whereas only 15 ppm HCN were produced with CuO(0.78). No HCN was detected for the catalyst with the highest copper loading, CuO(1.65). As observed for N_2O, addition of water to the feed gas (Feed 1w) eliminates HCN formation.

The formation of ammonia as a further byproduct is shown in Fig. 4 for Feed 1 (A) and Feed 1w (B). No ammonia was found for pure alumina in the temperature range investigated. A shift of the maximum NH_3 formation to lower temperatures similar to the shift for the formation of nitrogen (Fig. 2) can be observed with increasing

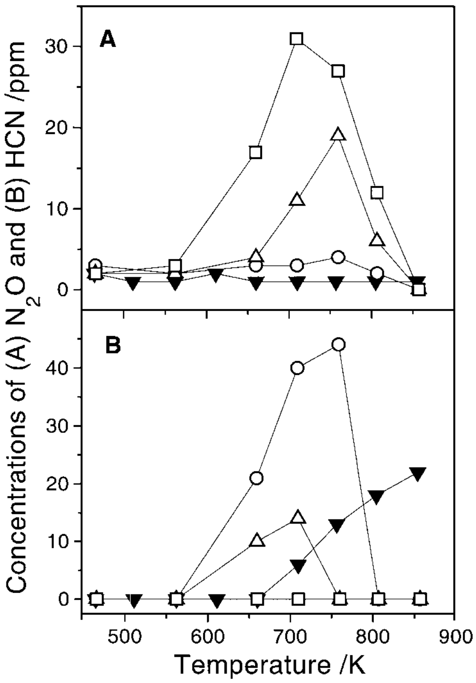

FIG. 3. Formation of (A) nitrous oxide and (B) hydrogen cyanide using Feed 1: (▼) Al_2O_3, (○) CuO(0.46), (△) CuO(0.78), and (□) CuO(1.65); total flow rate, 150 ml(STP)/min; catalyst weight, 250 mg.

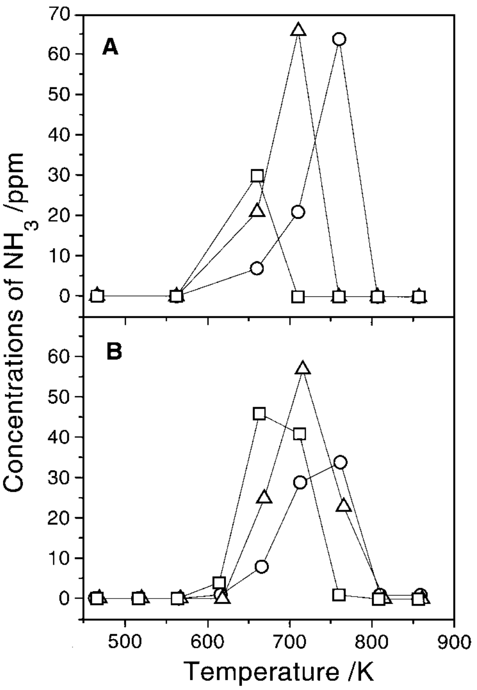

FIG. 4. Ammonia formation as a function of temperature for (A) Feed 1 and (B) Feed 1w: (○) CuO(0.46), (△) CuO(0.78), and (□) CuO(1.65); total flow rate, 150 ml(STP)/min; catalyst weight, 250 mg.

copper loading. Comparable maximum concentrations of ca. 65 ppm NH_3 were measured for catalysts CuO(0.46) and CuO(0.78), whereas 30 ppm were found for CuO(1.65). Addition of water to the system (Feed 1w) did not significantly alter the temperature range for maximum formation of ammonia, but the maximum concentration increased for the sample with highest copper loading, remained stable for CuO(0.78), and decreased for CuO(0.46).

Reduction of NO_2 by propene. When nitrogen dioxide (Feed 3) is used instead of nitric oxide, two new characteristics emerge for the formation of nitrogen. Pure alumina exhibits the highest activity, with the N_2 yield reaching 90% at 663 K, and pronounced low temperature activity is found for the copper-containing catalysts in the range 563–613 K (Fig. 5A). Interestingly, nitrogen formation does not seem to be influenced by the CuO loading in this temperature range. Above 613 K a behavior comparable to that of NO (Feed 1) is observed, with the maxima in N_2 formation being shifted to lower temperatures by ca. 50 K for the NO_2-containing feed. Note that NO_2 was only found below 613 K in the effluent gas for the CuO-loaded catalysts, whereas above this temperature NO_2 was completely converted to NO and N_2. With pure alumina, NO_2 was found below 662 K. Again, complete oxidation of propene to CO_2 and H_2O occurred at the temperature of the maximum nitrogen yield for the copper-containing catalysts. Although activity for nitrogen formation was markedly higher for

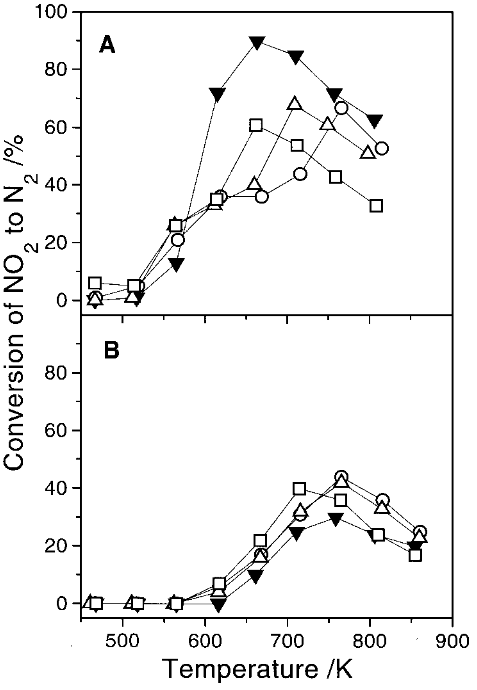

FIG. 5. Conversion of NO_2 to nitrogen as a function of temperature for (A) Feed 3 and (B) Feed 3w: (▼) Al_2O_3, (○) CuO(0.46), (△) CuO(0.78), and (□) CuO(1.65); total flow rate, 150 ml(STP)/min; catalyst weight, 250 mg.

pure alumina with Feed 3 compared to Feed 1, propene conversion was in the same range reaching a maximum of ca. 50% at 863 K, with CO being the prevailing product at higher temperatures.

Figure 5B illustrates the influence of water on the formation of nitrogen for the feed containing NO_2 and propene. Activity for nitrogen formation comparable to that with Feed 1w was observed for Feed 3w with copper-loaded catalysts, indicating that the presence of water levels off the influence of the nitrogen oxide used (NO or NO_2). A substantial decrease in the maximum nitrogen yield to 30% was observed for pure alumina when Feed 3w was used, but the N_2 yield was still superior to the value found for NO/propene.

With respect to the formation of nitrous oxide, hydrogen cyanide, and ammonia as byproducts, N_2O production was not affected by the use of either NO or NO_2 in the feed. Figure 6 shows the formation of HCN for Feed 3. On pure alumina, a maximum of 68 ppm was found at 565 K. For CuO(0.46) two maxima can be observed at 566 K (16 ppm) and at 709 K (19 ppm), which decrease with increasing CuO loading. Note that with NO no low temperature peak of HCN was found for the copper-containing catalysts. In the presence of water (Feed 3w) no HCN was formed on copper-loaded catalysts, whereas ca. 10 ppm HCN were produced at 623 K with pure alumina. As observed with NO/propene, ammonia formation was negligible over pure alumina in the temperature range investigated when dry NO_2/propene was used. For the copper-containing catalysts the formation of ammonia is depicted in Fig. 7. With NO_2 (Feed 3), a dependence of ammonia formation on copper loading similar to that for NO is observed. The maximum NH_3 concentrations of all samples (26 ppm at 708 K for CuO(0.46), 25 ppm at 661 K for CuO(0.78), and 8 ppm at 615 K for CuO(1.65)) are shifted to lower temperatures by ca. 40 K. Independent of the type of nitrogen oxide used, the maximum of ammonia peaks always at ca. 50 K lower temperature than the maximum nitrogen yield. This is also the case when a NO_2/propene feed containing water (Feed 3w) is used. Concentrations and temperature ranges of ammonia formation comparable to those with Feed 1w were observed (Fig. 7B compared with Fig. 4B), again pointing to an equalizing effect of water on the influence of the nitrogen oxide used (NO or NO_2).

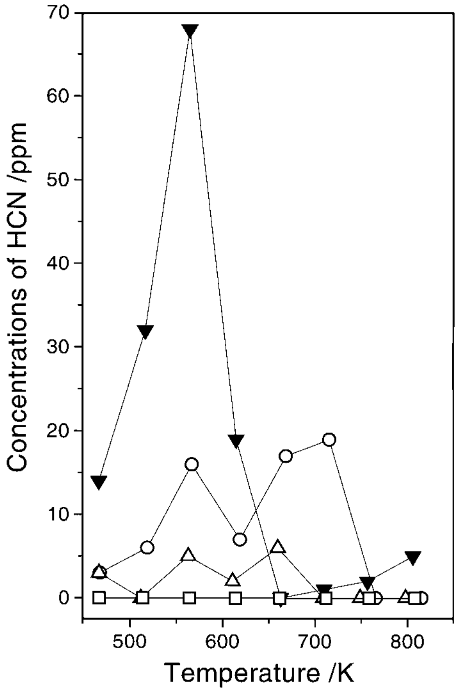

FIG. 6. Formation of hydrogen cyanide as a function of temperature using Feed 3: (▼) Al_2O_3, (○) CuO(0.46), (△) CuO(0.78), and (□) CuO(1.65); total flow rate, 150 ml(STP)/min; catalyst weight, 250 mg.

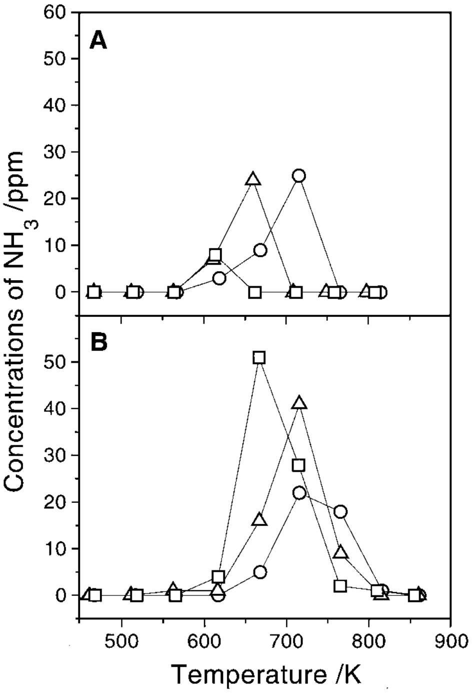

FIG. 7. Ammonia formation as a function of temperature for (A) Feed 3 and (B) Feed 3w: (○) CuO(0.46), (△) CuO(0.78), and (□) CuO(1.65); total flow rate, 150 ml(STP)/min; catalyst weight, 250 mg.

Reduction of NO and NO_2 by ethene. The use of ethene instead of propene as a reducing agent resulted in similar activities for the selective catalytic reduction of NO (Feed 2), as shown in Fig. 8A. For alumina as well as for the copper-loaded catalysts, essentially the same nitrogen yields as a function of temperature are obtained for dry feeds. Differences in catalytic behavior only became noticeable for the water-containing feed (Feed 2w), as emerges from Fig. 8B. With ethene, NO conversion to nitrogen reached ca. 30%, with the maxima shifted to temperatures ca. 100 K higher

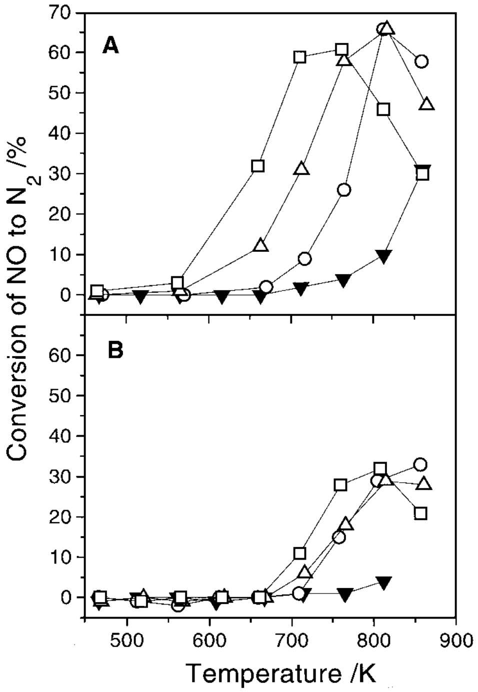

FIG. 8. Conversion of NO to nitrogen as a function of temperature for (A) Feed 2 and (B) Feed 2w: (▼) Al_2O_3, (○) CuO(0.46), (△) CuO(0.78), and (□) CuO(1.65); total flow rate, 150 ml(STP)/min; catalyst weight, 250 mg.

2% O_2/N_2. The sample loaded at 615 K showed the largest amount of gas phase products formed, indicating the highest loading of the catalyst with adsorbates or deposits. For loading temperatures exceeding 661 K a steady decrease in the amount of gaseous products was found that for 765 K, the temperature of maximum nitrogen yield during reaction with Feed 1 over CuO(0.78), only low concentrations of CO, CO_2, and NH_3 were measured, indicating an almost clean surface. Comparing the relative amounts of products formed, CO_2 and H_2O represent the highest proportion, followed by CO, and, with a maximum concentration of 45 ppm, NH_3. The temperatures of maximum formation of CO, CO_2, and NH_3 are comparable for identical loading temperatures and are shifted to higher temperatures for increasing loading temperatures. The temperature window of NH_3 formation during TPSR (Fig. 9B) coincides with the one observed in the catalytic tests (see Fig. 3).

No ammonia formation and substantially lower concentrations of CO (107 ppm at 648 K) and CO_2 (396 ppm at 679 K) were observed when CuO(0.78) was loaded with Feed 1w at 615 K. This indicates that the presence of water suppresses the formation of deposits on the catalyst surface, which moreover do not contain precursor species for NH_3 formation. TPSR experiments conducted with CuO(0.78) loaded at 615 K with a feed containing ethene (Feed 2) in place of propene resulted in less pronounced evolution than with propene. Using Feed 4 and 4w (NO_2/ethene) for catalytic tests further indicated that the type of hydrocarbon hardly influences the catalytic behavior of copper/alumina catalysts in the reduction of NO_x. As regards the formation of byproducts, comparable amounts of N_2O and significantly lower concentrations of HCN with a similar temperature dependence were measured when ethene was employed as reducing agent. The most stringent effect observed with the use of ethene instead of propene concerns the formation of ammonia, as no ammonia was found for feeds containing ethene.

Temperature-Programmed Surface Reactions of Adsorbed Species (TPSR)

In order to investigate the nature and amount of deposits formed on the catalyst under reaction conditions and their possible role in the formation of byproducts, sample CuO(0.78) was loaded with different feeds, rapidly cooled to 423 K in nitrogen, and subsequently heated in various atmospheres. The evolving products were analyzed by infrared analysis of the gas phase.

Figure 9 depicts the temperature dependence of the formation of CO, NH_3, and CO_2 for the TPSR in 2% O_2/N_2 using sample CuO(0.78) loaded with Feed 1 at 562, 615, and 661 K, respectively. Production of other gas phase products such as HCN or N_2O was negligible during TPSR in

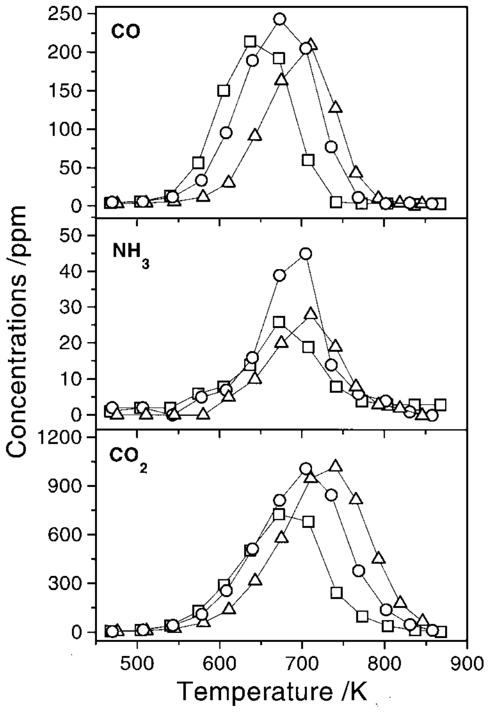

FIG. 9. Comparison of formation of carbon monoxide, ammonia, and carbon dioxide vs temperature for temperature-programmed surface reaction in 2% O_2/N_2 of CuO(0.78), loaded with Feed 1 at different temperatures: (□) loaded at 562 K, (○) loaded at 615 K, and (△) loaded at 661 K.

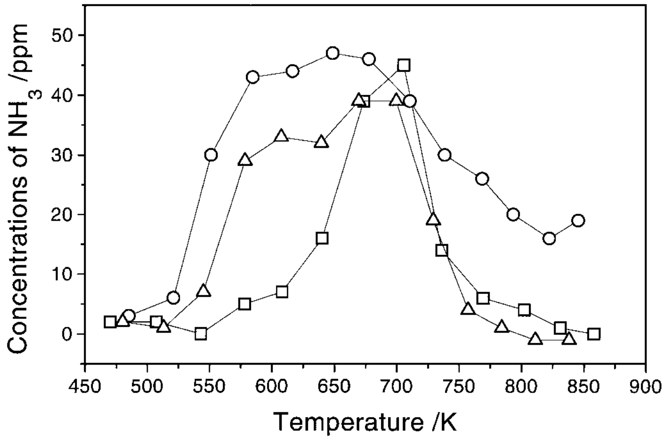

FIG. 10. Ammonia formation vs temperature during temperature-programmed surface reaction in various atmospheres over CuO(0.78) loaded at 615 K with Feed 1: (□) 2% O_2/N_2, (○) 2% H_2O/N_2, and (△) 2% $O_2 + 2\%$ H_2O/N_2; heating rate 10 K/min.

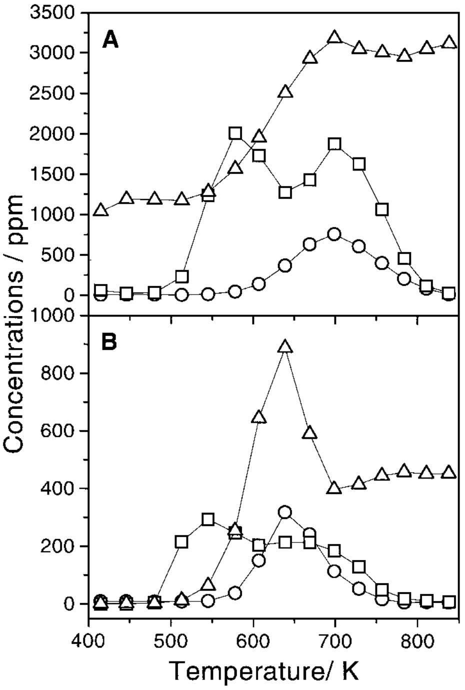

FIG. 11. Temperature-programmed reaction of (A) 1000 ppm ethyl isocyanate in 2% O_2 and (B) 212 ppm acetonitrile in 2% O_2 over CuO(0.78) pretreated at 873 K with 5% O_2/N_2 for 2 h and then cooled to 423 K, heating rate 10 K/min: (□) NH_3, (○) CO, and (△) CO_2.

of ammonia (7 ppm), as well as CO_2 (137 ppm) and CO (34 ppm), all at 652 K. Note that no ammonia was found in the catalytic tests with Feed 2.

Figure 10 shows the comparison of NH_3 evolution from CuO(0.78) loaded at 615 K with Feed 1 during TPSR in three different gas mixtures containing either O_2, H_2O, or $O_2 + H_2O$ as reactive components. With 2% H_2O/N_2, ammonia was produced over a wide temperature range starting at 520 K with a maximum of 47 ppm at 648 K. In the case of 2% O_2/N_2, ammonia appeared in the temperature range 584–811 K, peaking at 714 K with 45 ppm. Using both 2% O_2 and 2% H_2O in nitrogen two maxima were observed at 607 and 684 K, indicating two reaction pathways leading to NH_3. Table 2 lists the products observed during the TPSR experiments using different gas atmospheres, including 2% H_2/N_2.

In order to investigate the possibility of surface cyanide and/or isocyanate species being the primary source of ammonia formation, experiments were carried out using acetonitrile and ethyl isocyanate as model compounds. The concentrations of CO, CO_2, and NH_3 produced when 1000 ppm ethyl isocyanate was added to a TPSR feed containing 2% $O_2 + 2\%$ H_2O in nitrogen are depicted in Fig. 11A for CuO(0.78) pretreated for 2 h at 873 K in 5% O_2/N_2. Ammonia formation takes place in a temperature range (500–800 K) comparable to that found in Fig. 10 for the sample loaded with Feed 1. Furthermore, as in Fig. 10, two clearly discernible peaks of ammonia formation are observed at 575 K (2020 ppm) and at 700 K (1890 ppm). Carbon dioxide is produced over the whole temperature range investigated, whereas CO appears in the product gas

TABLE 2

Concentrations of Gas Phase Components during TPSR Measurements over CuO(0.78) Loaded with Feed 1 at 615 K

	TPSR with 2% O_2/N_2			TPSR with 2% H_2/N_2			TPSR with 2% $O_2 + 2\%$ H_2O/N_2		
Component	*T*-range [K]	*T*-maximum [K]	Max. Conc. [ppm]	*T*-range [K]	*T*-maximum [K]	Max. Conc. [ppm]	*T*-range [K]	*T*-maximum [K]	Max. Conc. [ppm]
NH_3	584–811	714	45	580–738	675	9	545–757	607/684	33/39
HCN	—	—	—	474–855	738	13	415–545	480	12
NO	714–811	779	19	417–611	440	34	—	—	—
CO	550–779	679	244	547–855	611	81	513–757	669	318
CO_2	517–874	714	1010	511–855	770	124	480–811	669	725
H_2O	445–874	646	539	474–855	547	569	—	—	—
C_2H_4	—	—	—	738–855	770	20	513–699	669	8

as a single peak at 700 K (770 ppm) simultaneously with the second NH_3 peak. In addition, a small amount of HCN with a maximum of 43 ppm at 640 K was detected. Note that this temperature lies between the two maxima of ammonia formation. A similar picture emerges when 212 ppm acetonitrile are used in place of ethyl isocyanate (Fig. 11B), with the evolution of ammonia starting at a slightly lower temperature (480 K). Two NH_3 peaks appear at 545 K (295 ppm) and at 640 K (216 ppm). Note that CO formation, peaking at 640 K (320 ppm), again overlaps with the second ammonia peak. The onset temperature for CO_2 and CO formation is shifted by ca. 60 K to higher temperatures compared to the NH_3 formation. The high concentrations found for the low temperature peak of ammonia, exceeding the feed concentrations of the isocyanate and nitrile species, indicate that reactions to adsorbates or deposits formed at lower temperatures are involved in the formation of NH_3.

Performing the same experiments with a reactant gas containing either 2% O_2 or 2% H_2O in nitrogen resulted in single ammonia peaks for the water-containing gas mixture (616 K for ethyl isocynate, 575 K for acetonitrile), whereas two ammonia peaks were observed for the oxygen-containing feed at temperatures comparable to the experiment with the water/oxygen containing feed (Fig. 11), but with the second peak being significantly lower.

To clarify whether ammonia formation could result from the hydrolysis of HCN, TPSR measurements with 2% H_2O/N_2 containing 200 ppm HCN were performed using pretreated CuO(0.78). Ammonia evolution started at 440 K and became stable at 700 K. Hydrogen cyanide was found in the gas phase up to 550 K. A maximum in CO_2 formation was observed at 580 K and CO appeared as a peak starting at 500 K with maximum at 650 K. Above this temperature the water-gas shift reaction became relevant, resulting in a decrease in CO and a concomitant increase in CO_2 formation.

TABLE 3

Reported Literature Data of IR Absorptions in the Spectral Range 1400 to 2400 cm^{-1}

Catalyst	Wavenumber (cm^{-1})	Species	Reference
—	2132.0, 2096.7	gaseous HCN	(45)
SiO_2	2105	adsorbed HCN	(46)
SiO_2	2298, 2265	adsorbed CH_3CN	
NiY-zeolite	2323, 2296, 2263	adsorbed CH_3CN	
Cu/ZSM-5	2260–2270	nitrile species	(41)
Cu, Cu–Cs/ Al_2O_3	2266, 2230	isocyanate on Cu/Al_2O_3	(21, 22)
	2262/2236 (shoulder)	isocyanate on alumina	
	2150	cyanide on Cu/Al_2O_3	
	1660	C=N structure of $NO_x \cdot C_yH_z$ complex	
Cu/Al_2O_3	2240	isocyanate species	(28)
Cu/Al_2O_3	2258, 2232	NCO, NCO^-	(44)
	2176, 2185	CO on Cu^{2+}	
	2118, 2135	two types of CO on Cu^+	
	2097	CO on Cu^0	
Al_2O_3	2250	NCO on alumina	(47)
Cu/Al_2O_3	2255–2260	NCO on Cu/Al_2O_3	
Cu/SiO_2	2230–2240	NCO on Cu^0	
	2200–2210	NCO on Cu^+	
	2185–2195	NCO on Cu^{2+}	
Cu/ZrO_2	2190	NCO species	(39)
	2140	CN species	
Noble metals/ Al_2O_3	2343, 2357	adsorbed carbon dioxide	(36)
	2232–2254	isocyanate species	
	2232	isocyanate on alumina	
	2125	cyanide species	
	1465, 1583	carbonate species	
Rh/Al_2O_3	2185	isocyanate on Rh	(40)
	2250	isocyanate on alumina	
Pt/Al_2O_3	1633	imine or substituted imine	(49)
	1472, 1564	carbonate	
	2261	isocyanate on Pt	
	2130	anionic $[NCO]^-$ or nitrile species	
Ce/ZSM-5	2266, 2241	two NCO species	(15)
	2112	adsorbed cyanide or NO_2	
	1658	organic nitrito species	
	1637	adsorbed water	

Diffuse Reflectance Infrared Fourier Transform (DRIFT) Measurements

Adsorption of pure compounds. Assignment of IR bands were made on the basis of values reported in the literature (Table 3) as well as by measuring the IR spectra of pure compounds (CO, HCN, CH_3CN, and C_2H_5NCO) adsorbed at 423 K on CuO(0.78) pretreated *in situ* in the chamber. Adsorption of CO resulted in the appearance of bands at 2135, 2120 (shoulder), 2102, and 2176 cm^{-1} (weak, broad), characteristic for adsorbed CO (44). Purging with nitrogen at 423 K weakened all bands until they disappeared. Simultaneously, bands of gaseous CO appeared in the spectra. Admission of 200 ppm HCN/N_2 to pretreated CuO(0.78) at 423 K produced a strong band at 2131 cm^{-1} with a shoulder at 2097 cm^{-1} assignable to gas phase or weakly adsorbed HCN (45). Simultaneously bands at 2161 and 2250 cm^{-1} with a shoulder at 2231 cm^{-1} appeared. Heating the sample in N_2 resulted in a continuous decrease of the bands at 2250 and 2231 cm^{-1} until both disappeared at 623 K. The band at 2161 cm^{-1} slightly increased and the band at 2131 cm^{-1} shifted to 2135 cm^{-1} and decreased up to 523 K. Further increasing the temperature resulted in a shift of these bands to 2145 cm^{-1} and 2117 cm^{-1}, respectively, at 683 K. The two bands remained stable even in the presence of 5% H_2/N_2 and are assigned to cyanide (CN) species adsorbed on the surface (15, 22, 36, 46), whereas the bands at 2250 and 2231 cm^{-1} are assigned to isocyanate (NCO) species (15, 22, 44, 47) formed by reaction of HCN with oxygen left on the catalyst surface after the pretreatment procedure. Upon injection of CH_3CN into a flow of nitrogen at 423 K three strong bands at 2328, 2298, and 2254 cm^{-1} were immediately observed, which are assigned to adsorbed acetonitrile (46). When the sample was heated in nitrogen, the bands disappeared above 423 K and two new weak bands grew at 2141 and 2117 cm^{-1} for temperatures exceeding 623 K, indicating thermal decomposition of adsorbed CH_3CN to surface-bound cyanide species. When ethyl isocyanate was used instead of acetonitrile no bands ascribable to adsorbed species in the range 2000–2400 cm^{-1} were observed at low temperatures. However, heating in nitrogen again produced bands at 2142 and 2117 cm^{-1} at 673 K, which became stronger at higher temperatures, and which are assigned to cyanide species.

DRIFT spectra of loaded catalysts. The spectral region between 2000 and 2400 cm^{-1} is emphasized in the following, as adsorbed species of interest in this work (nitriles, cyanides, isocyanates) generally have infrared absorptions in this frequency range. Figure 12 shows DRIFT spectra of CuO(0.78), loaded with Feed 1 at 615 K and cooled to ambient temperature in N_2, upon heating in a flow of 5% O_2/N_2. A band at 2233 cm^{-1} with a shoulder at 2241 cm^{-1} is observed at 423 K, indicating the formation of isocyanate species (Fig. 12B). At 523 K further bands appear at 2361, 2330, and 2117 cm^{-1} and in the range 2175–2140 cm^{-1}. The bands at 2361 and 2330 cm^{-1} are due to the formation of adsorbed CO_2 (36), whereas formation of a cyanide species is evidenced by the new bands at 2117 cm^{-1}. The bands observed are strongest at 553 K and then decrease upon further heating. Temperatures exceeding 553 K are characterized by the appearance of positive bands at 2206 cm^{-1} and around 2150 cm^{-1} (broad), indicative of the removal of surface species. At 773 K only positive bands at 2212 cm^{-1} and in the range 2175–2100 cm^{-1} are observable. In addition to the bands found in the spectral range 2000–2400 cm^{-1}, admission of 5% O_2/N_2 at 423 K caused the appearance of bands at 2993 and 2908 cm^{-1} (Fig. 12A) and at 1591 and 1390 cm^{-1} (Fig. 12C), which increased on further heating to 583 K. The bands are assigned to the formation of formate species (48). Simultaneously positive bands at 1647, 1576, and 1458 cm^{-1} emerged, indicating the disappearance of adsorbed water (10, 15), nitrito (10, 15, 37), or imine species (49) at 1647 cm^{-1} and of carbonate or carboxylate species (36, 49) at 1576/1458 cm^{-1}, respectively. Upon further heating the absorption bands associated with the formate species turned into positive bands (disappearing species) located at 3001, 2904, 1591, 1394, and 1377 cm^{-1}, whereas the bands at 1647, 1576, and 1458 cm^{-1} gained intensity. In the C–H region weak negative signals located at 3114, 2914, 2848, and 2770 cm^{-1} appeared in the DRIFT spectra (Fig. 12C), suggesting that H-containing species had been removed from the surface.

A different picture emerged when CuO(0.78) loaded with Feed 1 was heated in a flow of 5% H_2/N_2 (Fig. 13). Increasing the temperature to 523 K produced two bands at 2142 and 2116 cm^{-1}, indicating the formation of surface cyanide species (Fig. 13B). While the band centered at 2142 cm^{-1} steadily decreased for higher temperatures, the

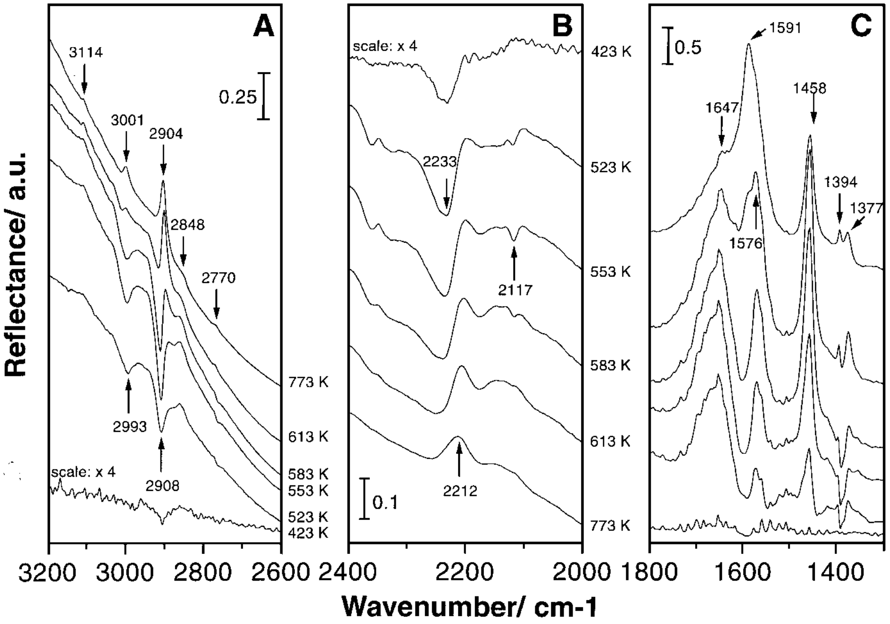

FIG. 12. Diffuse reflectance FTIR spectra at different temperatures recorded during temperature programmed experiments in 5% O_2/N_2 over CuO(0.78) loaded at 615 K with Feed 1.

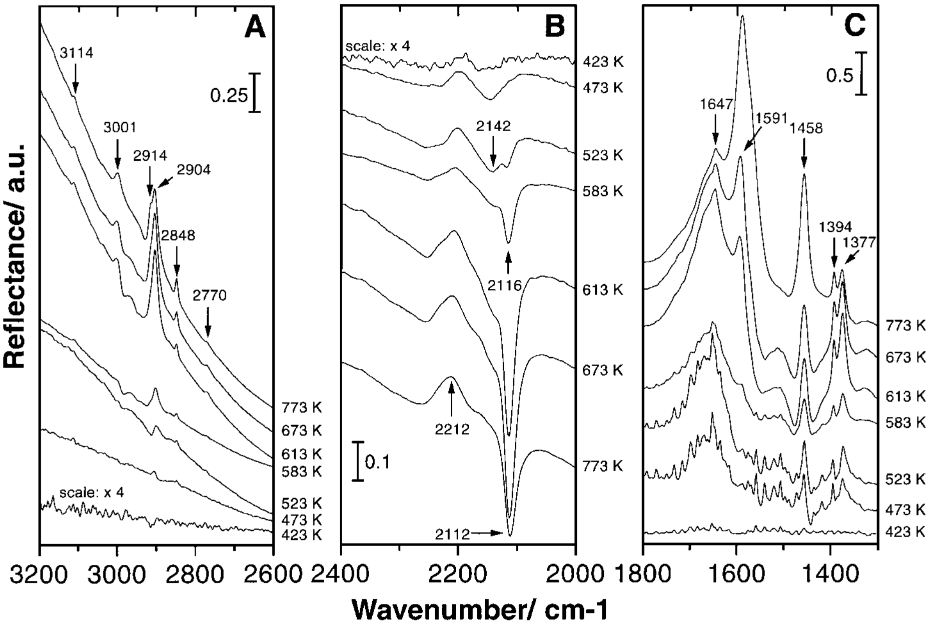

FIG. 13. Diffuse reflectance FTIR spectra at different temperatures recorded during temperature programmed experiments in 5% H_2/N_2 over CuO(0.78) loaded at 615 K with Feed 1.

band at 2116 cm^{-1} passed through a maximum at 613 K and then decreased above 673 K. The band which disappeared upon heating is tentatively assigned to a cyanide species adsorbed on the copper component and the stable band to CN species located on the alumina support. Assignment of the IR bands to cyanide and isocyanate species is supported by the finding that upon adsorption of hydrogen cyanide, acetonitrile, and ethyl isocyanate on CuO(0.78) the same surface species with absorptions at 2142 and 2116 cm^{-1}, assignable to surface CN-fragments, are observed at elevated temperatures in nitrogen, whereas absorptions due to adsorbed isocyanate species appeared at 2231 and 2250 cm^{-1} for HCN at lower temperatures (Table 4). Note that in the same temperature range HCN can be observed in the gas phase during the corresponding TPSR experiment in 2% H_2/N_2 (Table 2). A broad weak band with two maxima at ca. 2255 and 2235 cm^{-1} appeared at low temperatures and decreased upon further heating, turning into a positive band (removal of surface species) centered at 2212 cm^{-1}. Note that at 773 K the formation of a cyanide species is still evident (strong peak at 2112 cm^{-1}) and that the concomitant disappearance of a species with a band at 2212 cm^{-1} is observed. With regard to the spectral ranges between 2600 and 3200 cm^{-1} (Fig. 13A) and 1300 and 1800 cm^{-1} (Fig. 13C), no absorptions due to the formation of formate species were seen at low temperatures. At temperatures exceeding 523 K, bands characteristic for adsorbed water, nitrito or imine species (1647 cm^{-1}), formate species (3001, 2904, 1591, 1394, and 1377 cm^{-1}), and carbonate species (1576, 1458 cm^{-1}) disappeared, suggesting that the concomitant surface species have been removed from the surface. As observed with the corresponding TPO experiment, weak absorptions appeared at 3114, 2848, and 2770 cm^{-1}.

FTIR spectra of CuO(0.78) loaded with Feed 1w showed no absorptions in the spectral range 2000–2400 cm^{-1} upon

TABLE 4

Assignment of Observed IR Bands of Species Adsorbed on CuO(0.78)

Wavenumber/cm^{-1}	Tentative Assignment	Origin[a]
2102, 2120, 2135, 2176	adsorbed CO	CO adsorption
2135, 2161	cyanide species	HCN adsorption
2231, 2250	isocyanate species	HCN adsorption
2117, 2145	cyanide species[b]	HCN adsorption
2254, 2298, 2328	adsorbed CH_3CN	adsorption of acetonitrile
2117, 2141	cyanide species[b]	adsorption of acetonitrile
2117, 2142	cyanide species[b]	adsorption of ethyl isocyanate
2330, 2361	adsorbed CO_2	TPO
2233, 2241	isocyanate species	TPO
$2117^{(weak)}$	cyanide species	TPO
2116, 2142[c]	cyanide species	TPR
2212[d]	nitrile or isocyanate species	TPO, TPR
1377, 1394, 1591, 2904, 3001	formate species	TPO, TPR
1458, 1576	carbonate species	TPO, TPR
1647	nitrito-or imine species, or ads. NH_3	TPO, TPR

---

[a] TPO: heating in 5% O_2/N_2; TPR: heating in 5% H_2/N_2.
[b] Bands observed at elevated temperatures upon heating in nitrogen.
[c] Stable up to 773 K.
[d] Species removed from the surface at elevated temperatures.

heating in 5% O_2/N_2. Additionally, the intense band observed around 1647 cm^{-1} in the previous experiments remained weak, indicating that neither isocyanate nor cyanide species or their precursor species are deposited on the surface in the presence of water. Moreover, assignment of the band at 1647 cm^{-1} to adsorbed water is less probable, as similar concentrations were observed during the corresponding TPSR experiments. Similarly as with the sample loaded with Feed 1, bands due to formate species appeared above 423 K (2997, 2906, 1595, and 1390 cm^{-1}), which increased on further heating to 573 K and then disappeared. Concomitantly, carbonate species (1576, 1458 cm^{-1}) were removed. Note that no positive bands due to the removal of formate species were observed.

DISCUSSION

Catalytic Behavior

Catalytic tests clearly indicate that copper loading as well as reaction parameters significantly determine the performance of copper/alumina catalysts in NO_x reduction by olefins. Independent of the reaction parameters, the onset temperature as well as the temperature of maximum nitrogen formation shifted to lower values for increasing copper loadings and maximum nitrogen yield was slightly lower for sample CuO(1.65), with highest copper loading using dry feeds. The addition of copper to alumina was occasionally reported to lower the active temperature region of Al_2O_3 and to increase maximum catalytic activity for nitrogen formation (9, 19, 20). It was suggested that copper is active in the oxidation of NO to NO_2. Torikai *et al.* (20) observed maximum activity enhancement at relative low copper loadings of 0.3 wt%, implying that isolated copper ions are involved in the oxidation of NO to NO_2. The present results corroborate that for NO-containing feeds activity substantially increases as soon as copper is added to alumina (Fig. 2A). However, among the catalysts investigated, maximum activity is obtained for catalyst CuO(1.65) with 1.65 wt% CuO. Note that pure alumina exhibited highest activity for NO_x reduction when starting from feeds containing NO_2 (Fig. 5A). Comparing the selective reduction of NO with the corresponding reduction of NO_2 reveals that NO reduction occurs at markedly higher temperatures and to a lower extent for dry feeds, independent of the hydrocarbon employed as a reductant. This finding is in agreement with literature data, where NO_2 was frequently reported to be more reactive than NO in the selective reduction of NO_x (2, 30). Pronounced low temperature activity up to 613 K was observed for NO_2-containing feeds (Feeds 3 and 4), independent of the copper loading, which could be ascribed to the presence of NO_2 in the feed, as no NO_2 was measured in the product gas for temperatures exceeding 613 K. No important influence of the type of olefin on catalytic activity was found for dry feeds.

Water addition to the feeds suppressed NO_x reduction, with the effect being markedly more pronounced for pure alumina compared to the copper-containing catalysts. With CuO/Al_2O_3 catalysts, water addition resulted in similar behavior independent of the copper content but with CuO(1.65) still being most active. For these catalysts the use of either NO or NO_2 had no effect on nitrogen formation, with both reductants for feeds containing 10% water. Furthermore, NO_x reduction occurred at lower temperatures and to a higher extent for wet feeds with propene as reductant for both nitrogen oxides (NO, NO_2).

Formation of Byproducts

Like catalytic activity, formation of byproducts is strongly influenced by the copper loading and the feed composition. Ethene as a reductant generally showed a low tendency to form undesired byproducts, whereas significant amounts of N_2O, HCN, and NH_3 were observed for feeds containing propene. The formation of nitrous oxide is mainly affected by the copper loading and the presence of water. N_2O formation increases with increasing copper loading, suggesting that its formation occurs on sites involving copper species as N_2O was not observed over alumina. Water addition eliminates N_2O formation. Similarly, no hydrogen cyanide is found over the copper-containing catalysts for wet feeds, though 10 ppm HCN were measured over alumina with Feed 3w. Using dry feeds, substantial amounts of HCN were produced over alumina with both nitrogen oxides. For the copper/alumina catalysts HCN formation is more pronounced with NO and its concentration decreases with increasing copper loading, with CuO(1.65) showing no tendency to produce HCN. Ammonia formation is observed only in the presence of copper with the concentration decreasing with increasing copper loading for dry feeds. The influence of water on NH_3 formation is opposed, depending on the copper loading. For CuO(0.46) ammonia formation decreases in the presence of water, whereas markedly higher yields were obtained for CuO(1.65). Note that independent of the feed composition the maximum of ammonia peaks is always at ca. 50 K lower temperature than the maximum nitrogen yield.

Temperature-Programmed Surface Reactions of Adsorbed Species (TPSR)

Temperature-programmed surface reaction experiments were carried out to elucidate whether adsorbates or surface deposits formed under reaction condition are involved in N_2 formation and in the formation of nitrogen-containing byproducts such as NH_3 and HCN. Carbonaceous deposits were frequently reported to be involved in the selective reduction of NO by organic compounds over alumina (11, 32) as well as Cu/ZSM-5 (6). Obuchi *et al.* (32) suggested that NO is converted to N_2 through the formation of C–NO bonds at the carbon deposit by a radical reaction. The role of the catalyst is to promote the formation of carbon deposits from the reactant organic compounds by cracking or partial oxidation. Carbonaceous material containing nitrogen reacts with NO or NO_2 (50) as well as organic nitro or nitrite compounds formed from NO_x and propene (10, 12, 15, 37) were also proposed as intermediates, which are transformed to N_2. Surface isocyanate (22, 36, 39), cyanide (36, 39), and nitrile (41) species formed from NO_x and propene on various catalysts were reported to react with NO or NO_2, thus producing N_2. Recently, Poignant *et al.* (18) suggested that ammonia produced during the SCR of NO by propene in excess oxygen could play the role of an intermediate over Cu/ZSM-5. Using Cu/ZSM-5 to reduce NO_x with propylene, Bell *et al.* (8) observed at low temperatures, where NO_x reduction activity is low, carbonaceous deposits and organic isocyanates on the surface. The authors pointed out that these species are not representative of those being observed at the more relevant temperature of maximum NO_x reduction, where IR detects $Cu(N_xO_y)_z$ and $Cu{-}N_2$. Results obtained in this study also reveal that the amount and nature of species deposited under reaction conditions depends on temperature and reactant gas composition. Compared to lower loading temperatures, significantly less CO_2, CO, and NH_3 were measured during TPSR with samples loaded at the temperature of maximum catalytic activity. The use of wet feeds also suppressed the formation of deposits on the catalyst surface, which moreover do not contain precursor species for NH_3 formation, indicating that the presence of 10% water in the feed results in immediate hydrolysis of possible precursor species of NH_3, as ammonia is observed during catalytic tests with wet feeds. TPSR experiments with ethyl isocyanate and acetonitrile clearly show that hydrolysis of these compounds takes place in the same temperature range where NH_3 formation occurs during TPSR measurements, suggesting the participation of isocyanate and/or nitrile species in the mechanism of NH_3 formation. By investigating the interaction of NO and CO on the surface of Pt/Al_2O_3, Unland (49) earlier proposed a mechanistic pathway of ammonia formation via surface isocyanate species as intermediates and work by Voorhoeve *et al.* (51, 52) on the reaction of NO with CO and H_2 over noble metal catalysts showed that gaseous HCN an NH_3 are formed in the temperature range 673–1073 K. It was proposed that HCN could be formed via an intermediate surface isocyanate fragment by reduction with either H_2 or CO and that hydrolysis of the NCO group to NH_3 occurs on the Al_2O_3 support. Hydrogenation of the isocyanate complex to HCN is suggested to compete with hydrolysis to NH_3 (51, 52). This is in agreement with the present finding that no HCN is observed for wet feeds during catalytic tests and that HCN concentration exceeds NH_3 concentration for TPSR experiments with 2% H_2/N_2, whereas NH_3 is the prevailing product for TPSR in water-containing atmospheres (Table 2). TPSR experiments with 200 ppm HCN in 2% H_2O/N_2 moreover revealed that HCN is already hydrolyzed to NH_3 at 440 K over CuO(0.78), indicating that HCN either is not formed or is directly transformed to NH_3 under reaction conditions using wet feeds.

Recently it has been shown that gaseous HNCO is produced in the catalytic reduction of NO_x by olefins over Cu/ZSM-5 (16) as well as in the $CO/NO/H_2$ reaction over Pt/SiO_2 (55). No NHCO was obtained when Pt/Al_2O_3 was used under the same conditions or when Al_2O_3 was placed downstream of the Pt/SiO_2 catalyst (53). Gaseous HNCO could not be detected throughout this work, indicating that isocyanate species are mainly hydrolyzed to NH_3 and CO_2 on the alumina support, as ammonia was observed in the gas phase during catalytic tests as well as in TPSR experiments.

Diffuse Reflectance Infrared Fourier Transform (DRIFT) Measurements

DRIFT measurements were carried out in order to elucidate the nature and reactivity of IR observable adsorbates formed during the hydrocarbon–NO_x reaction. Table 4 summarizes the IR bands observed in this work. Straightforward assignment of vibrational absorptions in the range 2000–2400 cm^{-1} to adsorbed species with defined structure remains difficult. Nitriles (*R*–CN) show IR bands in the range 2190–2285 cm^{-1} (54) and organic isocyanates (NCO covalently bound) possess IR bands at 2269 ± 6 cm^{-1} (49), whereas transition metal isocyanate complexes (*M*–NCO) show IR absorbances in the range 2190–2240 cm^{-1} (54, 55). IR absorption frequencies of isocyanate species are furthermore reported to depend on the nature of the catalyst (55). Following NHCO adsorption on Cu/SiO_2, Solymosi and Bánsági (47) attributed absorption bands at 2230–2240 cm^{-1} to $Cu^0{-}NCO$, at 2200–2210 cm^{-1} to $Cu^+{-}NCO$, and at 2180–2185 cm^{-1} to $Cu^{2+}{-}NCO$. On Al_2O_3 and Cu/Al_2O_3 only one strong absorption band at 2255–2260 cm^{-1} was observed. Lower IR frequencies in the range 2105–2140 cm^{-1} are typically found for cyanide species (36, 39, 46), which furthermore depend on the binding character of the CN group, with ionic cyanides possessing absorptions around 2080 cm^{-1} (54).

Loading of CuO(0.78) with Feed 1 at 615 K followed by heating in either 5% O_2 (TPO) or 5% H_2 (TPR) in nitrogen resulted in the elimination of formate and carbonate species from the catalyst surface. In addition, surface isocyanate species were formed during TPO by reaction of a precursor species with oxygen, whereas heating the sample in 5% H_2/N_2 produced predominantly cyanide species. Unland (49) identified isocyanate species by isotopic labelling and infrared absorption experiments during the reaction of NO with CO over alumina-supported platinum catalysts. An absorption band at 2260–2270 cm^{-1}, which was assigned to an isocyanate species coordinated to the metal was observed

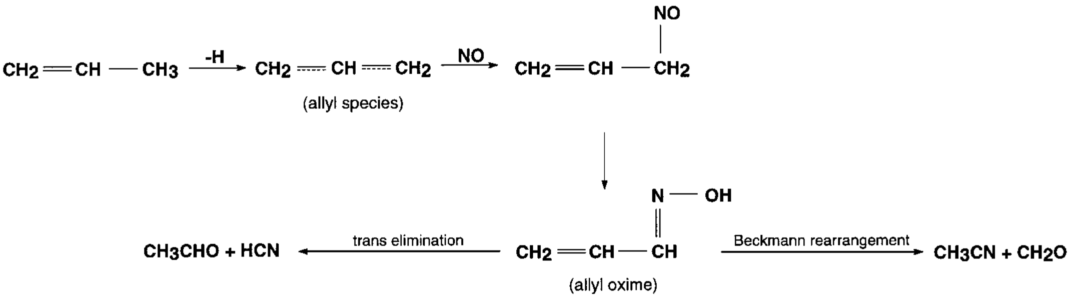

SCHEME 1

above 473 K. Similarly, Cu–NCO species were observed by London and Bell (56) using infrared spectroscopy in the catalytic reduction of NO by CO over Cu/SiO_2 catalysts. In their discussion of a possible reaction mechanism they postulated the formation of a copper nitride species (CuN), which can form Cu–NCO by reaction with CO.

As mentioned before, assignment of the positive bands at 1647 and 2212 cm^{-1} to species being removed from the surface at elevated temperatures during TPO and TPR experiments cannot unambiguously be made, as nitrile as well as organic isocyanate species show absorptions around 2200 cm^{-1} (49, 54). Hayes *et al.* (41) recently ascribed a band at 2260 cm^{-1}, appearing during the NO/propene reaction on Cu/ZSM-5, to an aliphatic cyanide species (nitrile), which could only be detected in the absence of oxygen. Large amounts of gaseous HCN, acetonitrile, and acrylonitrile were also observed in the oxygen-free reaction of NO with propene over Rh/Al_2O_3 (57). Assignment of the band at 1647 cm^{-1} to imine (49), organic nitrito (15), and oxime species (58) and to adsorbed water (15) or ammonia (46, 59) is possible. FTIR experiments of CuO(0.78) loaded with a wet feed (Feed 1w) showed no bands at 2212 cm^{-1} and only weak absorption at 1647 cm^{-1}. The finding indicates that a contribution from adsorbed water to the band at 1647 cm^{-1} is less probable. Moreover, no HCN and NH_3 were found during TPSR measurements of CuO(0.78) loaded with a wet feed, giving evidence that the species characterized by absorptions at 1647 and 2212 cm^{-1} are involved as precursors in the formation of HCN and NH_3.

The present results support a mechanism where HCN and NH_3 are formed from nitrogen-containing precursors, characterized by absorptions at 1647 and 2212 cm^{-1}, which react upon heating in H_2/N_2 to form cyanide surface species, whereas predominantly isocyanate surface intermediates appear when heating in O_2/N_2. Hydrolysis of the isocyanate intermediate provides a pathway to ammonia formation (49), whereas HCN can be formed by reduction of the surface isocyanate fragment with H_2 or CO (51, 52) or directly from the cyanide intermediate. By investigating the formation of byproducts in the ammoxidation of propylene, Menon (60) proposed a mechanism (Scheme 1) wherein an adsorbed allyl intermediate forms an allyl oxime by reaction with NO. Acetaldehyde and HCN are formed by *trans* elimination of the oxime species, whereas Beckmann rearrangement produces CH_3CN and CH_2O. On the basis of Scheme 1, the precursor species characterized by absorptions at 1647 and 2212 cm^{-1} are assigned to an oxime and a nitrile species, respectively.

CONCLUSIONS

The catalytic performance, as well as the formation of nitrogen-containing byproducts, in the selective catalytic reduction of NO_x by olefins in excess oxygen over copper/alumina is governed by the copper loading, the hydrocarbon used as a reductant (ethene, propene), the nitrogen oxide (NO or NO_2), and the presence of water. Increasing the copper loading results in a shift of the onset of nitrogen formation to lower temperatures and in slightly lower maximum activity. NO_2 is reduced more efficiently than NO with both reductants but with ethene showing a lower tendency to form HCN and NH_3. Water addition suppresses catalytic activity and formation of HCN and N_2O and levels off the influence of copper loading.

TPSR measurements with copper/alumina loaded with dry feeds revealed the presence of adsorbates or deposits leading to the evolution of CO, CO_2, and NH_3 when heated in O_2 and/or H_2O-containing atmospheres. No ammonia was observed for catalysts loaded with wet feeds. Reference TPSR experiments with acetonitrile or ethyl isocyanate in oxygen and/or water-containing atmospheres showed a temperature dependence of ammonia formation similar to that observed for the catalysts loaded under reaction conditions. FTIR investigation of a catalyst loaded with a dry NO/propene feed showed the disappearance of formate, carbonate, and nitrogen-containing species upon heating in H_2/N_2 or O_2/N_2. Surface isocyanate and cyanide species appeared as intermediates upon heating. No such species were observed for catalysts loaded with wet feeds. The findings indicate that ammonia is formed by hydrolysis of an isocyanate intermediate, whereas HCN is likely to be formed by reaction of the isocyanate intermediate with H_2 or CO or by direct reaction from the nitrogen-containing precursor, which is expected to be a nitrile or oxime species.

ACKNOWLEDGMENTS

The authors thank J. Weigel for the opportunity to carry out DRIFT measurements and for experimental assistance. Financial support of this work by the Nationaler Energie-Forschungs-Fonds (NEFF-Project 569) is gratefully acknowledged.

REFERENCES

1. Taylor, K. C., *Catal. Rev.-Sci. Eng.* **35**, 457 (1993).
2. Shelef, M., *Chem. Rev.* **95**, 209 (1995).
3. Iwamoto, M., Yahiro, H., Shundo, S., Yu-u, Y., and Mizuno, N., *Shokubai* **32**, 430 (1990).
4. Held, W., König, A., Richter, T., and Puppe, L., *SAE Tech. Pap. Ser.* **810**, 13 (1990).
5. Bennet, C. J., Bennett, P. S., Golunski, S. E., Hayes, J. W., and Walker, A. P., *Appl. Catal.* **86**, L1 (1992).
6. Ansell, G. P., Diwell, A. F., Golunski, S. E., Hayes, J. W., Rajaram, R. R., Truex, T. J., and Walker, A. P., *Appl. Catal. B* **2**, 81 (1993).
7. Burch, R., and Millington, P. J., *Appl. Catal. B* **2**, 101 (1993).
8. Bell, V. A., Feeley, J. S., Deeba, M., and Farrauto, R. J., *Catal. Lett.* **29**, 15 (1994).
9. Iwamoto, M., *Stud. Surf. Sci. Catal.* **84**, 1395 (1994).
10. Yasuda, H., Miyamoto, T., and Misono, M., *ACS Div. Petr. Chem.* **39**, 99 (1994).
11. Burch, R., and Scire, S., *Appl. Catal.* **3**, 295 (1994).
12. Yokoyama, C., and Misono, M., *J. Catal.* **150**, 9 (1994).
13. Bethke, K. A., Li, C., Kunk, M. C., Yang, B., and Kung, H. H., *Catal. Lett.* **31**, 287 (1995).
14. Cho, B. K., *J. Catal.* **155**, 184 (1995).
15. Yasuda, H., Miyamoto, T., and Misono, M., *ACS Symp. Ser.* **587**, 110 (1995).
16. Radtke, F., Koeppel, R. A., and Baiker, A., *J. Chem. Soc. Chem. Commun.*, 427 (1995).
17. Radtke, F., Koeppel, R. A., and Baiker, A., *Catal. Today* **26**, 159 (1995).
18. Poignant, F., Saussey, J., Lavalley, J. C., and Mabilon, G., *J. Chem. Soc. Chem. Commun.*, 89 (1995).
19. Hamada, H., Kintaichi, Y., Sasaki, M., Ito, T., and Tabata, M., *Appl. Catal.* **75**, L1 (1991).
20. Torikai, Y., Yahiro, H., Mizuno, N., and Iwamoto, M., *Catal. Lett.* **9**, 91 (1991).
21. Ukisu, Y., Sato, S., Murmatsu, G., and Yoshida, K., *Catal. Lett.* **11**, 177 (1991).
22. Ukisu, Y., Sato, S., Muramatsu, G., and Yoshida, K., *Catal. Lett.* **16**, 11, (1992).
23. Miyadera, T., *Appl. Catal. B* **2**, 199 (1993).
24. Ukisu, Y., Sato, S., Abe, A., and Yoshida, K., *Appl. Catal. B* **2**, 147 (1993).
25. Iwamoto, M., Mizuno, N., and Yahiro, H., *Stud. Surf. Sci. Catal.* **75**, 1287 (1993).
26. Jen, H. W., and Gandhi, H. S., *ACS Symp. Ser.* **552**, 53 (1994).
27. Shelef, M., Montreul, C. N., and Jen, H. W., *Catal. Lett.* **26**, 277 (1994).
28. Hoost, T. E., Laframboise, K. A., and Otto, K., *Appl. Catal. B* **7**, 79 (1995).
29. Kintaichi, Y., Hamada, H., Tabata, M., Sasaki, M., and Ito, T., *Catal. Lett.* **6**, 239 (1991).
30. Hamada, H., Kintaichi, Y., Sasaki, M., Ito, T., and Tabata, M., *Appl. Catal.* **70**, L15 (1991).
31. Sato, S., Yu-u, Y., Yahiro, H., Mizuno, N., and Iwamoto, M., *Appl. Catal.* **70**, L1 (1991).
32. Obuchi, A., Ogata, A., Mizuno, K., Ohi, A., Nakamura, M., and Ohuchi, H., *J. Chem. Soc. Chem. Commun.*, 247 (1992).
33. Hamada, H., Kintaichi, Y., Yoshinari, T., Tabata, M., Sasaki, M., and Ito, T., *Catal. Today* **17**, 111 (1993).
34. Subramanian, S., Kudla, R. J., Chun, W., and Chattha, M. S., *Ind. Eng. Chem. Res.* **32**, 1805 (1993).
35. Radtke, F., Koeppel, R. A., and Baiker, A., *Catal. Lett.* **28**, 131 (1995).
36. (a) Bamwenda, G. R., Obuchi, A., Ogata, A., and Mizuno, K., *Chem. Lett.*, 2109 (1994). (b) Bamwenda, G. R., Ogata, A., Obuchi, A., Oi, J., Mizuno, K., and Skrzypek, J., *Appl. Catal. B* **6**, 311 (1995).
37. Tanaka, T., Okuhara, T., and Misono, M., *Appl. Catal. B* **4**, L1 (1994).
38. Burch, R., Millington, P. J., and Walker, A. P., *Appl. Catal. B* **4**, 65 (1994).
39. Li, C., Bethke, K. A., Kung, H. H., and Kung, M. C., *J. Chem. Soc. Chem. Commum.*, 813 (1995).
40. Anderson, J. A., and Rochester, C. H., *J. Chem. Soc. Faraday Trans. 1* **85**, 1117 (1989).
41. Hayes, N., Grünert, W., Hutchings, G., Joyner, R., and Shpiro, E., *J. Chem. Soc. Chem. Commun.*, 531 (1994).
42. Schneider, H., Tschudin, S., Schneider, M., Wokaun, A., and Baiker, A., *J. Catal.* **147**, 5 (1994).
43. Weigel, J., Koeppel, R. A., Baiker, A., and Wokaun, A., submitted for publication.
44. Hierl, R., Urbach, H.-P., and Knözinger, H., *in* "Proceedings, 10th International Congress on Catalysis, Budapest, 1992" (L. Guczi, F. Solymosi, and P. Tétényi, Eds.), p. 2697. Akademiai Kiadó, Budapest, 1993.
45. Jones, L. H., "Inorganic Vibrational Spectroscopy." Dekker, New York, 1971, p. 69.
46. Kiselev, A. V., and Lygin, V. I., "Infrared Spectra of Surface Compounds." J. Wiley, New York, 1975.
47. Solymosi, F., and Bánsági, T., *J. Catal.* **156**, 75 (1995).
48. Chauvin, C., Saussey, J., Lavalley, J.-C., Idriss, H., Hindermann, J.-P., Kiennemann, A., Chaumette, P., and Courty, P., *J. Catal.* **121**, 56 (1990).
49. Unland, M. L., *J. Phys. Chem.* **77**, 1952 (1973).
50. Yogo, K., Ono, T., Ogura, M., and Kikuchi, E., *in* "207th National Meeting ACS, San Diego, March 13–18, 1994," *Preprints Div. Pet. Chem.*, p. 159.
51. Voorhoeve, R. J. H., Trimble, L. E., and Freed, D. J., *Science* **200**, 759 (1978).
52. Voorhoeve, R. J. H., Patel, C. K. N., Trimble, L. E., Kerl, R. J., and Gallagher, P. K., *J. Catal.* **45**, 297 (1976).
53. Dümpelmann, R., Cant, N. W., and Trimm, D. L., *Appl. Catal. B* **6**, L291 (1995).
54. Nakamoto, K., "Infrared and Raman Spectra of Inorganic and Coordination Compounds," Wiley, New York, 1986.
55. Matyshak, V. A., and Krylov, O. V., *Catal. Today* **25**, 1 (1995).
56. London, J. W., and Bell, A. T., *J. Catal.* **31**, 96 (1973).
57. Mizuno, K., Kamuki, T., and Suzuki, M., *Chem. Lett.*, 731 (1980).
58. Clerc, J. T., Pretsch, E., and Seibl, J., "Studies in Analytical Chemistry," Vol. 1, "Structural Analysis of Organic Compounds by Combined Application of Spectroscopic Methods." Elsevier, Amsterdam, 1981.
59. Unland, M. L., *J. Catal.* **31**, 459 (1973).
60. Menon, P. G., *J. Catal.* **59**, 314 (1979).